JOURNAL OF SOLID STATE CHEMISTRY **98**, 415–422 (1992)

A Study of the Mass Transport Properties of the Solid State Copper(I) ion Conductor $Rb_4Cu_{16}I_7Cl_{13}$ and its Application in the Determination of the Thermodynamic Stability of Nd_2CuO_4

T. E. WARNER

Interdisciplinary Research Centre in Superconductivity,
University of Cambridge, Cambridge, CB3 OHE, United Kingdom

P. P. EDWARDS*

School of Chemistry, University of Birmingham, Edgbaston, Birmingham,
B15 2TT, United Kingdom

AND W. C. TIMMS AND D. J. FRAY

Department of Materials Science and Metallurgy, University of Cambridge,
Cambridge, CB3 3QZ, United Kingdom

Received November 28, 1990; in revised form January 2, 1992

The preparation of $Rb_4Cu_{16}I_7Cl_{13}$ from the respective metal halides in flowing argon is described. The electrochemical behavior of the solid state cell $Cu|Rb_4Cu_{16}I_7Cl_{13}|Cu$ has been studied by impedance spectroscopy. The electronic resistance of the external circuit is significant and is taken into consideration in the evaluation of the ionic conductivity. $Rb_4Cu_{16}I_7Cl_{13}$ has a copper ion conductivity of 69 Sm^{-1} at 473 K, and an activation energy of 14 kJ $mole^{-1}$ in the temperature range 351 to 473 K. Titration of copper through the cell revealed interesting morphological features of copper crystal growth at 473 K. EMF measurements on the cell $Cu|Rb_4Cu_{16}I_7Cl_{13}|Nd_2CuO_4$, Nd_2O_3, O_2, Pt gave $\Delta G° = -27{,}300 - 61\,T$ J $mole^{-1}$ K^{-1} for the cell reaction $Cu(c) + 0.5\,O_2(g) + Nd_2O_3(c) = Nd_2CuO_4(c)$.

Introduction

In 1979, Takahashi *et al.* (*1*) reported the discovery of a new copper(I) ion solid electrolyte, $Rb_4Cu_{16}I_7Cl_{13}$. They showed that this compound had a high copper ion conductivity of 34 Sm^{-1} at 298 K, and activation energies for conduction of 7.0 kJ $mole^{-1}$ between 403 and 248 K, and 19 kJ $mole^{-1}$ between 248 and 133 K. The transport number for the copper ion was considered to be near unity. Powder X-ray diffraction analysis showed that the crystal structure of $Rb_4Cu_{16}I_7Cl_{13}$ is simple cubic with lattice parameter $a = 1.002$ nm. Later work by Nag and Geller (*2*) indicated that there is a solid-solution range $Rb_4Cu_{16}I_{7+x}Cl_{13-x}$ with $(-0.6 < x < 1)$. Tokumoto *et al.* (*3*) have found this range

---

* To whom correspondence should be addressed.

0022-4596/92 $5.00

to be $0 < x < 0.5$, while Takahashi *et al.*(*4*) have proposed $-0.2 < x < 0.5$ as the solid-solution range.

Application of this ion conductor to thermodynamic EMF measurements in the Cu–Se system have been reported by Takahashi *et al.* (*5*) and by Chen *et al.* (*6*). The use of $Rb_4Cu_{16}I_7Cl_{13}$ in the control and determination of copper activity in the Chevrel compound $Cu_xMo_6S_{8-y}$ ($0 < y < 0.4$) by the construction of the solid-state electrochemical cell $Cu|Rb_4Cu_{16}I_7Cl_{13}|Cu_xMo_6S_{8-y}$, Pt, at 400 K is reported by Mizusaki *et al.* (*7*).

Takahasi *et al.* (*1*) synthesized $Rb_4Cu_{16}I_7Cl_{13}$ by an *in vacuo* technique using purified RbCl, CuCl, and CuI as starting materials. In this present study it is shown that this stoichiometric phase can be successfully prepared in relatively large amounts by a simplier route involving heating appropriate amounts of metal halides in an alumina boat in an atmosphere of flowing argon.

The present investigation involves a re-evaluation of the ionic conductivity of $Rb_4Cu_{16}I_7Cl_{13}$ as a function of temperature while taking into account the electronic resistance of the external circuit (platinum foil and wires), which is shown here to be significant at high temperatures. A higher frequency range was utilized in the impedance spectroscopy study, which enabled ionic conductivities to be measured with high accuracy.

Experimental

Synthesis

A 30-g sample of $Rb_4Cu_{16}I_7Cl_{13}$ was prepared by the following method. Starting materials included rubidium chloride (99.9%), copper(I) chloride (99.99%), and copper(I) iodide (99.99%), all supplied by Aldrich Chemical Co., Ltd. The appropriate molar ratio amounts of RbCl, CuCl, and CuI were weighed on a Metler 100 balance (±0.5 mg) and ground together with an agate pestle and mortar to a fine powder. In order to promote the reaction, this material was pressed into pellets of 13 mm diameter using a Specac stainless steel die under a pressure of 220 MPa. The pellets were placed in an alumina boat which was inserted inside a Lenton LTF12 horizontal tube furnace. The sample was heated to 503 K in a flowing argon atmosphere for 1 hr (i.e., just below the incongruent melting point), followed by annealing at 423 K for 24 hr before cooling to ambient temperature.

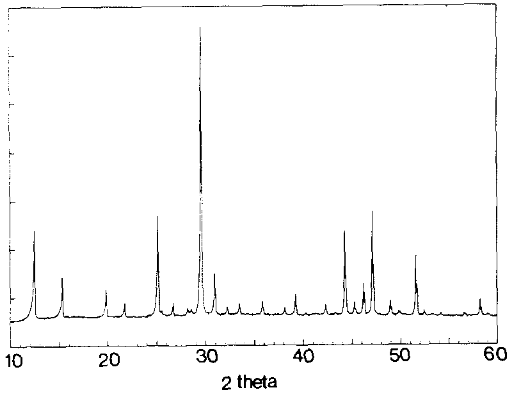

FIG. 1. X-ray powder diffraction pattern of $Rb_4Cu_{16}I_7Cl_{13}$ product material.

The appearance of the annealed pellets was white. The powder X-ray diffraction (XRD) pattern of the sample as obtained with a standard Philips diffractometer is shown in Fig. 1. The radiation was Cu*Kα* of wavelength 0.15418 nm. The crystal lattice spacings are attributed solely to $Rb_4Cu_{16}I_7Cl_{13}$ (*8*). This material was reground and pressed into 13-mm-diameter pellets of varying thicknesses, and reannealed at 423 K in flowing argon for 24 hr, followed by slow cooling to ambient temperature. The desired composition was again confirmed by powder XRD. The $Rb_4Cu_{16}I_7Cl_3$ pellet density is 87% of the theoretical density based on powder XRD lattice parameters. Therefore, the Cu(I) ionic conductivity values might be as high as ~1.15 times those calculated from the impedance data.

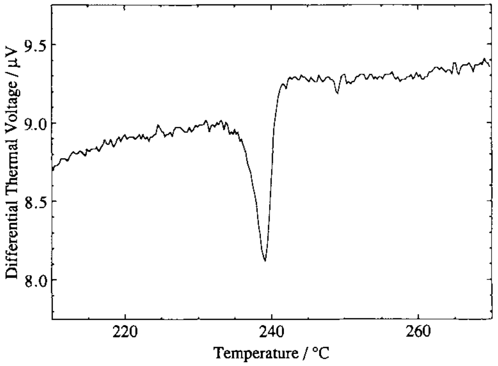

FIG. 2. Differential thermal analysis trace of $Rb_4Cu_{16}I_7Cl_{13}$.

Differential thermal analysis (DTA) of a 16-mg sample of the product material was performed with a Stanton Redcroft STA1500 simultaneous thermogravimetric analyzer/differential thermal analyzer, in flowing argon. Figure 2 shows an endothermic peak at 512 ± 3 K which corresponds to the incongruent melting point as reported by Takahashi *et al.* (*1*).

Pellets containing 95% Nd_2CuO_4 + 5% Nd_2O_3 were synthesized by standard methods as described in an earlier paper by Warner *et al.*(*9*).

Electrical Measurements

The total electrical conductivity was measured by impedance spectroscopy (I.S.). A computer-controlled data/capture treatment system was used by interfacing an EG&G PAR Model 273 potentiostat together with a Solatron 1255HF frequency response analyzer to an Amstrad PC1640 HD20 personal computer; 388M I.S. software was supplied by EG&G Instruments, Ltd. allowing measurements to be made in the frequency range 0.01 Hz to 100 kHz.

The conductivity cell composed of a pellet of $Rb_4Cu_{16}I_7Cl_{13}$ (13 mm diameter and various lengths) whose faces were ground flat with 1200-grit silcon carbide paper. This was then sandwiched between two flat pieces of copper foil (0.5 mm thick):

$$Cu|Rb_4Cu_{16}I_7Cl_{13}|Cu.$$

Satisfactory cohesion between the $Rb_4Cu_{16}I_7Cl_{13}$ pellet and the copper foil electrodes was achieved by annealing the cell (while under mechanical pressure) at 473 K for 3 hr prior to electrical measurements. This cell was held tightly between two platinum disks within a hollow rig machined from a piece of the ceramic Macor, using a spring for maintaining a force of approximately 10 N across the cell; 0.5-mm-diameter platinum wire insulated inside alumina sheaths provided the electrical connection to the rest of the external circuit. The temperature of the cell was measured with a type K thermocouple supplied by RS Components, Ltd. All I.S. measurements were carried out under an atmosphere of flowing argon (purified over copper) between 291 and 473 K. EMF measurements were determined with a Keithley Electrometer Model 614.

Results and Discussion

The impedance spectra for the reversible symmetric cell $Cu|Rb_4Cu_{16}I_7Cl_{13}|Cu$ at various temperatures in argon are shown in Fig. 3. The high-temperature impedance spectra are interpreted in terms of a Warburg impedance (i.e., a combination of bulk ionic resistance and Faradaic impedance). Therefore the interception at the real axis when this plot is extrapolated to infinite frequency (Re Z_∞) is taken as the ionic resistance of the bulk electrolyte in a series combination with the electronic resistance of the external circuit (i.e., platinum electrodes and wire). It is interesting to note the large inductance at 100 kHz for the high-temperature spectra. However, at lower temperatures the occurance of a semicircle at the high-frequency end of the spectra is interpreted in terms of grain boundary ionic resistance within the electrolyte pellet. The point

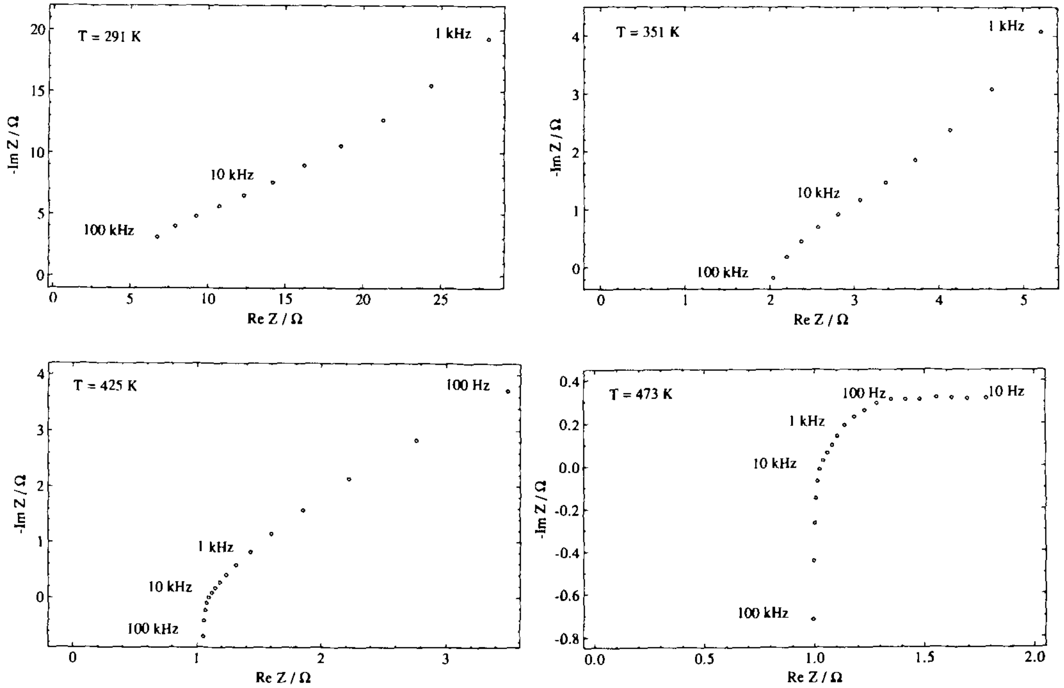

FIG. 3. Impedance spectra for the cell: Cu|$Rb_4Cu_{16}I_7Cl_{13}$|Cu at various temperatures.

where the high-frequency end of this semicircle intercepts the real axis is taken as the ionic resistance of the bulk electrolyte in series combination with the electronic resistance of the external circuit. However, at temperatures below 325 K, this extrapolation is not possible, due to the lack of data above 100 kHz. The results of a study of the effect of the thickness of the electrolyte pellet on the value of Re Z_∞ at 473 K are shown in Fig. 4. The value of Re Z_∞ extrapolated to zero length corresponds to the electronic resistance (0.62 Ω) of the external circuit at 473 K. There are intrinsic problems in elucidating accurate ionic impedance data in systems such as this, where the ionic resistance is of the same order of magnitude as the electronic resistance of the external circuit.

Takahashi *et al.* (*1*) performed electrical conductivity measurements on a similar cell to the one in this paper (albeit with composite copper/$Rb_4Cu_{16}I_7Cl_{13}$ electrodes). Their results are presented within the lower-frequency range of 400 Hz to 10 kHz, and without consideration of the electronic resistance of the external circuit. They display the frequency dependence of their data for temperatures between 299 and 392 K in the

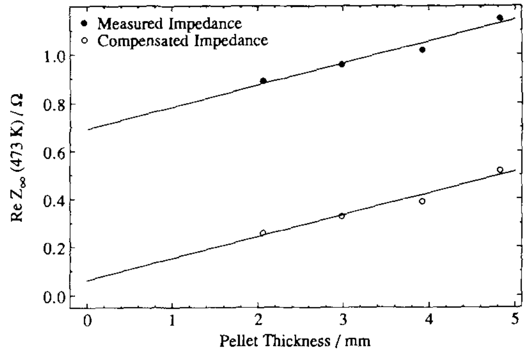

FIG. 4. Re Z_∞ as a function of pellet thickness.

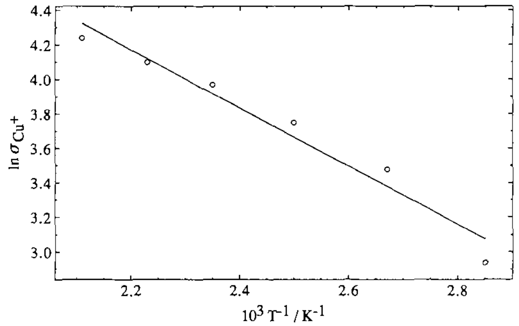

FIG. 5. Arrhenius plot for $Rb_4Cu_{16}I_7Cl_{13}$.

form of the plot Re Z versus $f^{-1/2}$ and attribute the linearity of this plot to a Warburg impedance. However, their assumption that this behavior extends to high frequencies (especially at low temperatures) has been shown in this current work to be invalid due to the occurrence of a semicircle at low temperatures. Therefore, the extrapolation of their plots to infinite frequency appears to yield inaccurate values for the bulk ionic resistance.

In this present work, the ionic conductivity of the bulk electrolyte was determined as a function of temperature and found to obey the Arrhenius law $\sigma = \sigma_0 \exp(-E_a/RT)$ in the temperature range 351 to 473 K (see Fig. 5). The activation energy (E_a) was calculated as 14 kJ $mole^{-1}$, which is double the value reported by Takahashi *et al.* (*1*) as 7.0 kJ $mole^{-1}$ for the range 248–403 K.

To demonstrate the high ionic conductivity of this electrolyte, titration of copper through the cell was performed at 473 K in an argon atmosphere. A constant current density of 377 Am^{-2} (based on the geometric area of the electrode) was passed through the cell for 3040 sec, corresponding to the titration of 100 mg of copper. The cell potential during the titration rose from approximately 50 to 60 mV. Once the titration was complete, the cell was cooled to ambient temperature and was inspected. A dendritic deposit of copper had occurred at the cathode, with extensive growth extending into the electrolyte. Figure 6 shows a scanning electron microscope (SEM) image of the cathode. Higher magnification revealed the extremely fine nature of the copper follicles, which appear to possess slip lines in the structure. The deposition is clearly nonuniform, with the reductive nucleation site penetrating into the solid electrolyte during the course of the reaction.

The thermodynamic data for Nd_2CuO_4 are required for an understanding of the phase stability relations in the Nd–Cu–O system, which is of importance in the synthesis of the n-type superconductor $Nd_{2-x}Ce_x CuO_4$ discovered recently by Tokura *et al.* (*10*). For this purpose EMF measurements were performed on the following electrochemical cell:

$$\mathrm{Cu}|\mathrm{Rb_4Cu_{16}I_7Cl_{13}}|95\%\ \mathrm{Nd_2CuO_{4-x}},\ 5\%\ \mathrm{Nd_2O_3},\ \mathrm{O_2(g)},\ \mathrm{Pt}.$$

This cell can be treated as a cell of the second kind, i.e., the cell EMF is indirectly dependent on the partial pressure of oxygen at the right-hand electrode, which defines the oxygen stoichiometry in Nd_2CuO_{4-x} and thereby determines the activity of copper in this phase. The cell reaction is

$$\mathrm{Cu(c)} + 0.5\mathrm{O_2(g)} + \mathrm{Nd_2O_3(c)} = \mathrm{Nd_2CuO_4(c)}.$$

If oxygen is present in the standard state (i.e., at 101 kPa) then $\Delta G^\circ_R = -nFE^\circ_{cell}$ applies, where n is the number of equivalents of charge passed through the external circuit (in this case $n = 1$).

However, in an atmosphere of any significant partial pressure of oxygen, the copper metal in the reference electrode will have a tendency to oxidize to Cu_2O (*11*). This by itself will not effect the above interpretation of the cell EMF since, provided that some copper is present in the electrode such that Cu and Cu_2O are at equilibrium, then the chemical potential of Cu in each phase is by definition identical, such that the reference Cu activity remains constant.

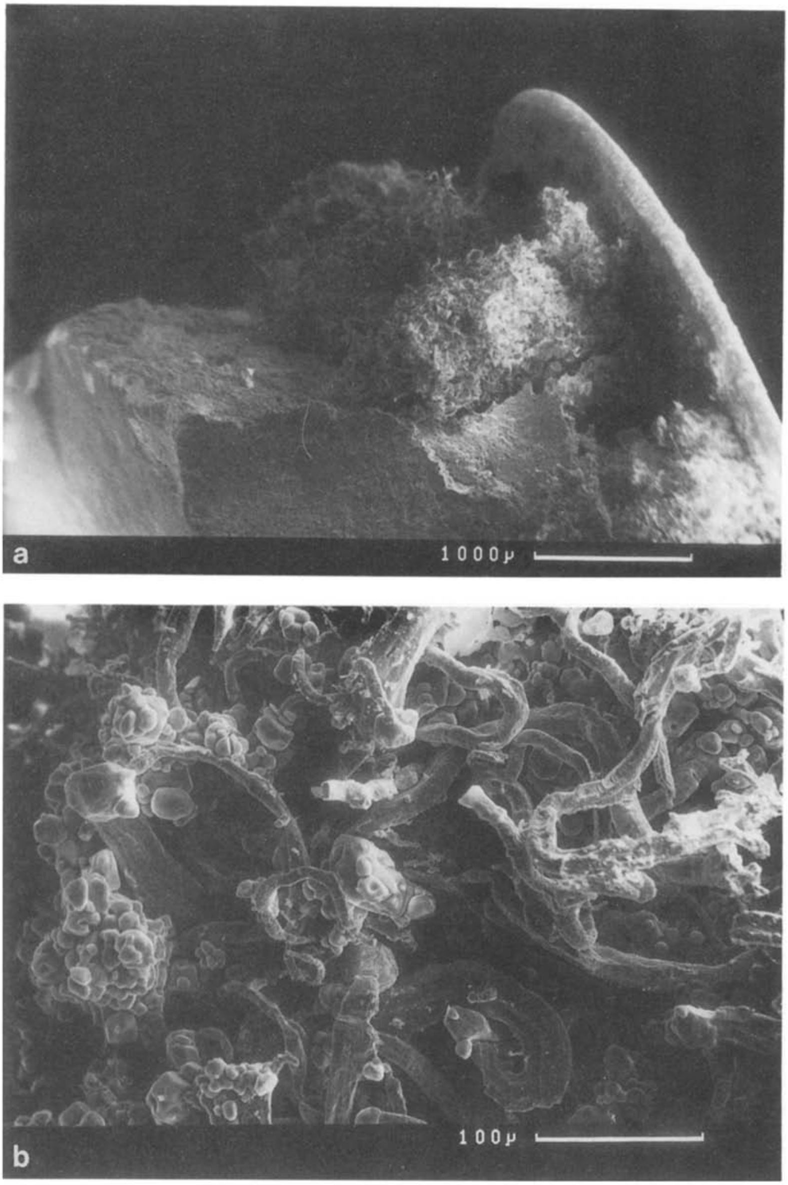

FIG. 6. Scanning electron microscope images of the cathodic copper deposit.

However, more severe oxidation to CuO will reduce the activity of Cu in the reference electrode and thereby make the above interpretation of the cell EMF inappropriate.

For these reasons the above cell was constructed and thermal equilibrium was brought about in an argon atmosphere. When the desired temperature was obtained the atmosphere was then changed to flowing oxygen (101 kPa). This caused the cell EMF to increase significantly. Once this remained steady (typically within 2–4 h) the cell EMF

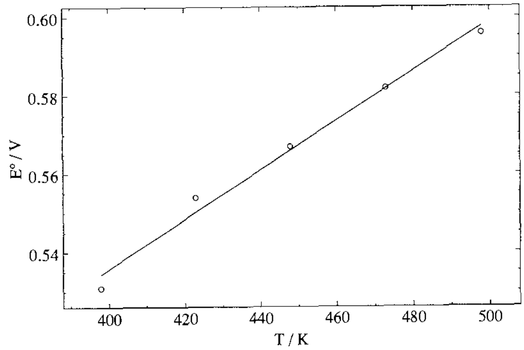

FIG. 7. Plot of standard EMF as a function of temperature for the cell: $Cu|Rb_4Cu_{16}I_7Cl_{13}|Nd_2CuO_4$, Nd_2O_3, O_2, Pt.

was recorded. Figure 7 shows the standard cell EMF as a function of temperature in the range 400 to 500 K. The entropy change for the cell reaction was determined from the linear temperature dependence of the cell EMF in this temperature region and was found to be 61 J mole^{-1} K^{-1}. This gave the following expression for the standard free energy change for the cell reaction:

$$\Delta G^\circ_R(400\text{–}500\ \text{K}) = -27300 - 61\ T\ \text{J mole}^{-1}\ \text{K}^{-1}.$$

It is noted that after several hours in a pressure of 101 kPa oxygen, and particularly at higher temperatures, that both the $Rb_4Cu_{16}I_7Cl_{13}$ electrolyte and copper reference electrode oxidize to CuO. This limits the life time of the cell, but nonetheless useful EMF measurements can be obtained in the early stages of the experiment.

Conclusions

$Rb_4Cu_{16}I_7Cl_{13}$ can be prepared successfully by a relatively simple route from commercially available high-purity material without recourse to purification procedures of starting material, and without the tedious use of sealed evacuated reaction conditions.

From the reversible cell $Cu|Rb_4Cu_{16}I_7Cl_{13}|Cu$, the impedance spectra reveal that for temperatures below 351 K frequencies > 100 kHz are required for an accurate determination of the ionic resistance of the electrolyte. The electronic resistance of the external circuit is significant and needs to be considered in evaluating the ionic resistance from the impedance spectra. Further work is being conducted at higher frequencies (10 MHz) to gain a better resolution of bulk and grain boundary resistances.

$Rb_4Cu_{16}I_7Cl_{13}$ has been found to be a suitable electrolyte for thermodynamic EMF measurements on Nd_2CuO_4 with respect to copper metal, in the temperature range 400–500 K. The standard free energy change for the reaction $Cu(c) + 0.5O_2(g) + Nd_2O_3(c) = Nd_2CuO_4(c)$ within this temperature range is $-27{,}300 - 61\ T$ J mole^{-1} K^{-1}. However, $Rb_4Cu_{16}I_7Cl_{13}$ is prone to oxidation in a significant partial pressure of oxygen, particularly at high temperatures.

Acknowledgments

The authors thank the Science and Engineering Research Council (SERC) of the United Kingdom for providing funds for this research. We are grateful to Dr. I. Gameson for the XRD pattern, and Mr. A. R. Jones for the DTA trace. One of the authors (T.E.W.) thanks Miss J. L. MacManus for the many interesting discussions concerning this work and for help in setting up the I. S. system.

References

1. T. TAKAHASHI, O. YAMAMOTO, S. YAMADA, AND S. HAYASHI, *J. Electrochem. Soc.* **126,** 1654 (1979).
2. K. NAG AND S. GELLER, *J. Electrochem. Soc.* **128,** 2670 (1981).
3. M. TOKUMOTO, N. OHNISHI, Y. OKADA, AND T. ISHIGURO, *Solid State Ionics* **3–4,** 289 (1981).
4. T. TAKAHASHI, R. KANNO, Y. TAKEDA, AND O. YAMAMOTO, *Solid State Ionics* **3–4,** 283 (1981).
5. T. TAKAHASHI, K. KUWABARA, M. MIURA, AND M. NAKANISHI, *J. Appl. Electrochem.* **12,** 213 (1982).
6. L. CHEN, Z. ZHAO, R. XUE, AND G. WANG, *Solid State Ionics* **9–10,** 1223 (1983).

7. J. MIZUSAKI, S. HAN, K. FUERI, AND K. KITAZAWA, *Solid State Ionics* **11,** 293 (1984).
8. International Centre for Diffraction Data, "Powder Diffraction File," Index Card 37-1206.
9. T. E. WARNER, P. P. EDWARDS, AND D. J. FRAY, *in* "Conference Proceedings, ICMC'90 Topical Superconductors—Materials Aspects, May 9–11, 1990, Garmisch-Partenkirchen, Germany."
10. Y. TOKURA, H. TAKAGI, AND S. UCHIDA, *Nature* **337,** 345 (1989).
11. C. E. WICKS AND F. E. BLOCK, "Thermodynamic Properties of 65 Elements," Bulletin 605 U.S. Bureau of Mines, Washington, DC (1963).